International Journal of Architectural, Civil and Construction Sciences
ISSN: 2415-1734
Vol:6, No:2, 2012

Tension Stiffening Parameter in Composite Concrete Reinforced with Inoxydable Steel: Laboratory and Finite Element Analysis

S. Alih and A. Khelil

Abstract**—**In the present work, behavior of inoxydable steel as reinforcement bar in composite concrete is being investigated. The bar-concrete adherence in reinforced concrete (RC) beam is studied and focus is made on the tension stiffening parameter. This study highlighted an approach to observe this interaction behavior in bending test instead of direct tension as per reported in many references. The approach resembles actual loading condition of the structural RC beam. The tension stiffening properties are then applied to numerical finite element analysis (FEA) to verify their correlation with laboratory results. Comparison with laboratory shows a good correlation between the two. The experimental settings is able to determine tension stiffening parameters in RC beam and the modeling strategies made in ABAQUS can closely represent the actual condition. Tension stiffening model used can represent the interaction properties between inoxydable steel and concrete.

Keywords**—**Inoxydable steel, Finite element modeling, Reinforced concrete beam, Tension-stiffening.

I. Introduction

INOXYDABLE steel is used in construction works for multiple reasons. Apart from their excellent resistance to corrosion, its high ductility is advantageous with respect to energy dissipation in the case of cyclic loading. Inoxydable steel from austenitic type is studied to determine their behavior as reinforcement bar in composite concrete beam. Focus is made on the interaction behavior with concrete and the tension stiffening phenomenon. This study highlighted a simplified approach to observe this interaction behavior in bending test instead of direct tension as per reported in many references. Their possibility to observe the tension stiffening behavior in composite concrete beam is then determined. FEA is conducted using ABAQUS software to verify the material model and laboratory results. Modeling strategies to simulate the actual condition of laboratory work is also elaborated. The constitutive laws, experimental work concept, and the FEA strategies used in this study could benefit future research in inoxydable steel and composite concrete.

S. Alih is a Doctorate in Civil Engineering in Nancy University, IUT Nancy Brabois, France; on leave from the Faculty of Civil Engineering, Universiti Teknologi Malaysia Skudai (e-mail: sophiacalih@yahoo.com).

A. Khelil is a Professor in Civil Engineering in Nancy University IJL UMR 7198 CNRS – Equipe 207, IUT Nancy Brabois CS 90137 F54601 Villers Les Nancy, France (phone: +333-83682536; fax: +333- 83682532; e-mail: abdel.khelil@iutnb.uhp-nancy.fr).

II. Inoxydable Steel In Composite Concrete Beam

In reinforced concrete structures, the presence of steel necessitates the consideration of bar-concrete interaction. The bar-concrete adherence allows the concrete located between cracks to resist tensile stresses, thereby reducing the average reinforcement stress level compared to its magnitude at the crack. This phenomenon results in a gain in rigidity, called tension stiffening.

A simple way to account for this local phenomenon is to integrate the bar-concrete interaction in a global dimension by modifying the stress-strain relationship of the material, either the reinforcing bar or the concrete. In this study, the tension stiffening model is integrated with concrete. It is describe and validated in detail in Reference [1]. Referring to Fig. 1, tension stiffening is described as the stress difference $\sigma_{S,TSE}$ between the steel stress σ_S of the reinforced concrete member and the stress $\sigma_{S,II}$ of bare steel at a given strain The stress increase $\sigma_{S,TSE}$ can be replaced by an equivalent concrete stress $\sigma_{C,TSE}$ which can be determined as [2],

$$\sigma_{C,TSE} = \rho_{eff}\sigma_{S,TSE} \quad (1)$$

where,

$$\sigma_{S,TSE} = (\sigma_S - \sigma_{S,II}) \quad (2)$$

$$\rho_{eff} = A_s / A_{c,eff} \quad (3)$$

ρ_{eff} is the effective reinforcement ratio, A_s is sectional area of the steel, and $A_{c,eff}$ is the effective zone of concrete around the re-bars which can be determine according to [3].

The stress-strain curve for reinforced concrete under uniaxial tension can be divided in three regions; pre cracking, crack development stage, and post cracking [4] as shown in Fig. 1(a). Before cracks start to form (pre cracking), concrete are able to resist tensile stress. These results in a higher stress level in concrete as shown in Fig. 1(b). When cracks start to form (crack development stage), concrete slowly looses their ability to resist tensile stress and so the stress level decreases. With the increase in formation of cracks (post cracking), stress in concrete decreases and more stresses will be carried by the reinforcement bars. Reinforcement stress level increases evidently after the formation of cracks.

This tension stiffening phenomenon has been observed experimentally by numbers of researchers through a uniaxial tension test. Most of these researches involved the study of concrete reinforced with construction steel and fiber-reinforced polymer (FRP) material. However, due to the difficulties of conducting the direct tension test, only limited and often conflicting results are available. More so, beam

subjected to uniaxial tension is unlikely to exist compared with bending. In this study, the possibility of observing tension stiffening phenomenon in a concrete structure subjected to bending is investigated. A similar concept of sample preparation with study conducted for uniaxial tension test is applied. A series of strain gauges are attached to the austenitic steel bar in tension zone to record changes in stress when load is applied. These changes is analyze and observe closely particularly during the phase before and after cracking. LVDT is placed at the center of the beam to record the central deflection.

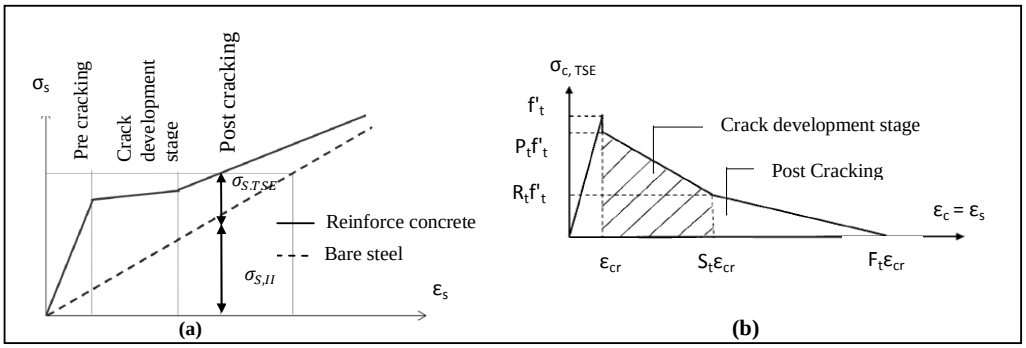

Fig. 1 Tension stiffening model derived from uniaxial tension (a), and the equivalent concrete stress-strain relationship (b): [2], [4], [5].

A. Preparation and Testing of Beam Sample

Fig. 2 shows the dimension of the reinforced concrete beam sample used in this study.

Two austenitic steel 20mm in diameter is used as the reinforcing bars in tension zone, and two carbon steel 8mm in diameter is used in compression zone. For this test, only austenitic-hot is use. 10 shear links formed from 6mm mild steel bars were provided at 70mm and 120mm from each ends for shear reinforcement in the shear spans. The beam were tested on simply supported condition with a clear span of 2.9m and loaded symmetrically and monotically.

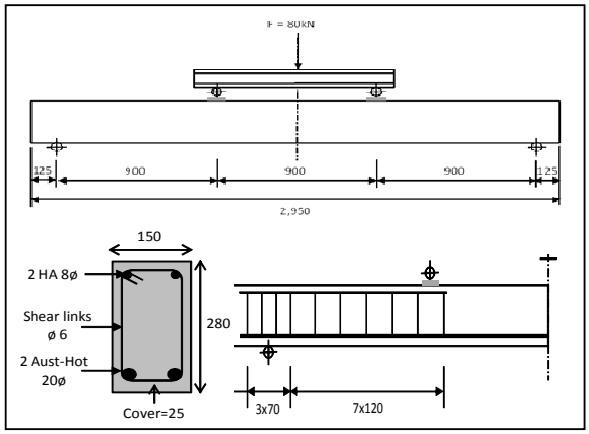

Fig. 2 Dimension of the RC beam as per constructed and tested in laboratory

Crushing test on the concrete sample in accordance with Reference [3] were conducted to identify the compressive strength of the concrete; f_c = 50 MPa, and the Young's Modulus of the concrete is 37,565 MPa.

As for the settings to study the tension stiffening behavior, a series of strain gauges are attached along the austenitic steel bars. Since the strain gauges were attached on the bar surface, the quantity has to be limited to minimize surface interferences. Therefore an effective number of strain gauges and the right position to place it have to be estimated prior. For this, a moment distribution diagram of the simply supported beam is used to predict the internal stress distribution as shown in Fig. 3(a). It can be observed that the stress distribution will increase between point A-B and will be identical with D-C. A total of six strain gauges were used and placed along the reinforcement bar at the position as shown in Fig. 3(a). It is marked as J1, J2, J3, J4, J5, and J6.

Fig. 3(b) shows the detail arrangement made on the strain gauges position. It is alternately positioned between the two bars to minimize the surface interferences and at the same time permit the changes in strain to be recorded in a close distances along the bar. Strain gauges marked as J2, J4, and J6 were placed along Bar 1, while J1, J3, and J5 were placed along Bar 2. When observed on the side view of the beam; these alternately positioned strain gauges will develop a series of strain gauges closely distance with each other along the beam member. The strain pattern can then be observed at different distance and load history.

B. Tension Stiffening Phenomenon

Tension stiffening phenomenon is observed with the increase of strain recorded along the reinforcement bars when load is applied. Tension stiffening can be viewed as an increase in stress on reinforcement bar when cracks start to form due to the inability of concrete to resist tensile stress. Analyzing the readings of strain gauges attached to the bars, the stress curve is plotted for the applied load; Fig. 4(a). Stress is determine by multiplying the strain values with elastic modulus of the austenitic steel; 177,305 MPa (based on tensile test conducted on the steel sample), assuming the steel is still in its limit of elasticity when 80 kN load is applied. For all six strain gauges, an increase of readings is recorded between 27 and 44 kN applied load. These increment can be view in two phases as shown in the figure. Taking J4 as example, a linear increase is recorded between 0 kN to 27 kN, followed by a

higher increase of stress between 27 kN to 80 kN. This sudden increase in strain and therefore the stress, shows the tension stiffening phenomenon as could be observed in direct tension test. All strain gauges shows the same increment pattern for the same range of load. This is when cracks is forming in the concrete beam.

J4 shows the highest reading (370 MPa) followed by J3 (320 MPa) for 80 kN applied load. This is due to their position in the center of the beam when deflection is maximum and crack formation is earlier. This is followed by J2 and J5, in which both reading shows close resemblance. J6 and J1 shows the lowest reading and close resemblance between each other as well. This proves the assumption that internal stress distribution will be identical for the two gauges if their position is identical from each end as shown in Fig. 3(a). Readings from the strain gauges interact well with theoretical assumption and shows the tension stiffening behavior for the beam sample.

Fig. 4(b) shows the strain pattern plotted along the reinforcement bar to investigate the strain distribution for the simply supported beam when load is applied. It can be observed that strain increases identically from both ends and maximum values are recorded in the center of the beam. When 30 kN load is applied, increase in strain is higher. Formation of cracks and deflection at the center gives higher values in the strain. This observation is similar when compared to the findings from direct tension test conducted in Reference [4]. When strain pattern is plotted along the reinforcement bar, higher strain increase is observed at the crack position.

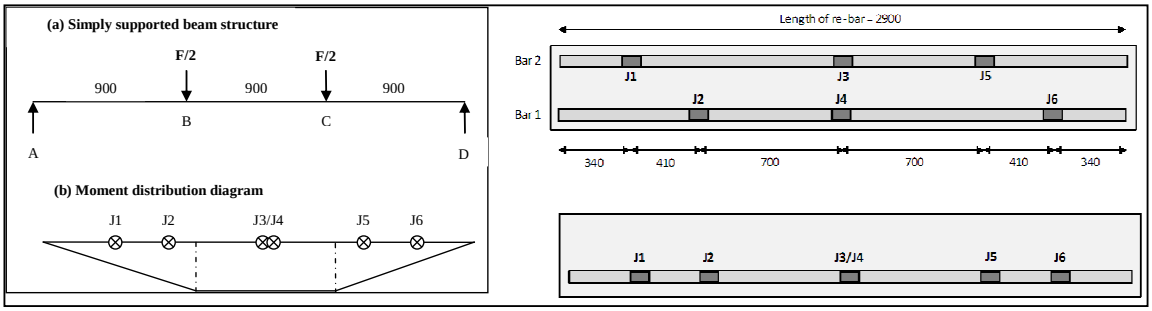

Fig. 3 Strain gauges position: (a) Determination based on moment distribution of the simply supported beam, (b) detail position along the bars

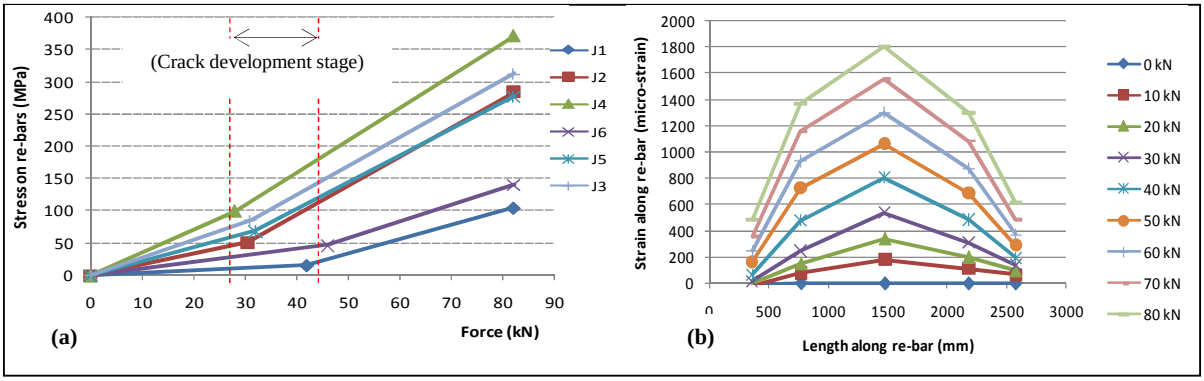

Fig. 4 Laboratory results: (a) Stress in each strain gauges for the applied force, (b) Strain pattern along the reinforcement bar recorded during laboratory test

III. Nonlinear Finite Element Analysis

A general purpose finite element code, Abaqus/Standard (STD), is utilized in this study. The traditional Newton-Raphson method (Static General) is applied together with the variety of routines for material models (concrete and steel), boundary conditions, interaction properties, and bond behavior.

A. Finite Element Modeling Strategies

Three-dimensional finite element analysis is conducted to examine the behavior of composite concrete structural elements internally reinforced with inoxydable steel. Concrete is modeled using 8-node 3-D solid elements while the internal reinforcement bars are modeled using 2-node embedded bar formulation in the concrete elements. By this approach, the reinforcing bars are treated as integral parts of the concrete element to determine the total internal resisting forces that are directly added to those of concrete.

Beam is modeled as simply supported with two point loads in the middle of the span. The loads are distributed evenly in a constraint area to avoid localized damage in one point. Loading's arrangement and dimension of the beam model is as shown in Fig. 2. Position of each strain gauges; J1, J2, J3, J4, J5, and J6 are marked precisely along the main reinforcement bar base on their actual position in beam sample of laboratory work; Fig. 5(a). History output results are generated on each position of the strain gauges to compare the values with the one recorded during experimental works.

The model is then meshed vertically into small elements so that each of the concrete elements contains re-bar. Little or no reinforcement in elements often introduces mesh sensitivity in the analysis results in the sense that the finite element prediction do not converge to a unique solution. The interaction between the re-bars and the concrete tends to reduce the mesh sensitivity.For the reinforcement bars, the model is develop with two austenitic steel 20mm in diameter in tension zone, two carbon steel 8mm in diameter in compression zone, and 10 shear links formed from 6mm mild steel bars were provided at 70mm and 120mm from each ends for shear reinforcement in the shear spans. Austenitic-hot is used as per laboratory work. Tensile test results are applied in the material properties for the reinforcement bar so their nonlinear plastic response could be accurately simulated in the numerical model. The reinforcement bars are modeled as embedded element in the concrete as shown in Fig. 5(b). These elements are superposed on the mesh of plain concrete elements. This modeling approach allows the concrete behavior to be considered independently of the rebar [6]. The smeared crack model provided in Abaqus/STD for plain concrete is applied to the FEA model. Tension stiffening is used to model the effects associated with the rebar/concrete interface.

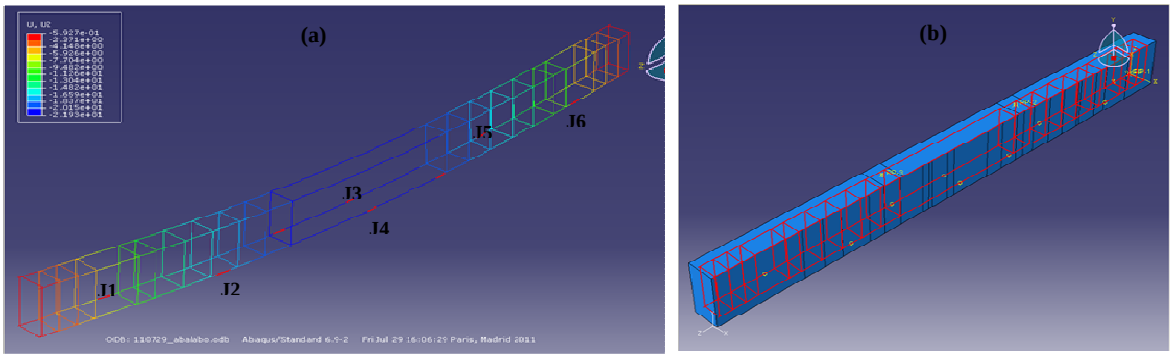

Fig. 5 Position of each strain gauges marked along the re-bar model (a), reinforcement bars modeled as embedded in concrete element (b).

B. Tension Stiffening Effect

The effect from rebar/concrete interface is approximated by introducing the tension stiffening, which simulates load transfer through the rebar across cracks. Tension stiffening effect is applied in the simulation by changing the material properties in concrete model rather than the reinforcement bars. Tension stiffening model develop by [5] as shown in Fig. 1(b) is used. These model involved four parameters; P_t, R_t, S_t, F_t together with the character of concrete; f'_t and ε_{cr} where

$$f'_t = 0.3 f_{ck}^{\left(\frac{2}{3}\right)} \quad (4)$$

$$\varepsilon_{cr} = \frac{f'_t}{E} \quad (5)$$

These concrete character is determine based on a compression test conducted on the concrete used to develop the concrete beam discussed in previous section, f_{ck} = 50 MPa, and E = 37,565 MPa. Therefore, the material model is based on the actual properties of the concrete beam. Values of the four parameters P_t, R_t, S_t, F_t are taken as 0.8, 0.45, 4, and 10 respectively. Fig. 6 shows the tension stiffening model applied to the simulation.

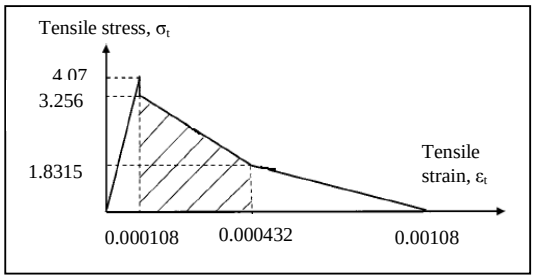

Fig. 6 Tension stiffening model applied to the finite element model

C. Comparison of Experimental and Numerical Results

Based on the history output results generated for each strain gauges; J1, J2, J3, J4, J5, and J6, a stress-strain curve for each strain gauges is plotted and compared to the results obtained from laboratory test. These results are verified by extracting the reinforcement bars frame from the composite model as shown in Fig. 5(a). Stress values for the identical positioned gauges resemble closely; J3 and J4, J2 and J5, J1 and J6. The internal stress distribution as shown in Fig. 7 can be better observed in these results. J3 and J4 shows the highest values of stress throughout the loading process; 400MPa for 80kN load. This is due to their position at the center of the beam where maximum deflection occurred

which leads to earlier formation of cracks. This is followed by J2 and J5 with 300MPa for the maximum load. J1 and J6 shows the lowest stress; 150MPa for 80kN of applied load.

Results from this numerical FEA are then compared with readings on strain gauges recorded in the experimental works as shown in Fig. 7 (b)-(d). In general, the result shows a good correlation between the FEA and experimental results. Values from numerical analysis are slightly higher than the one obtained from laboratory works. Comparison with the experimental works is made based on the set of strain gauges that provide similar readings due to their position along the bar. J4 and J3 are compared together in Fig. 7(b), comparison of J2 and J5 in Fig. 7(c), while J1 and J6 is compared in Fig. 7(d). Stress values from FEA for J3 and J4 are 50MPa higher than the experimental works when maximum load is applied. For J2 and J5, 25MPa difference in stress is observed for the 80kN load. J1 and J6 show a closer resemblance values in stress recorded through experimental and FEA. For all sets of gauges, increase in stress recorded in FEA is earlier than laboratory; 22kN where cracks starts to form.

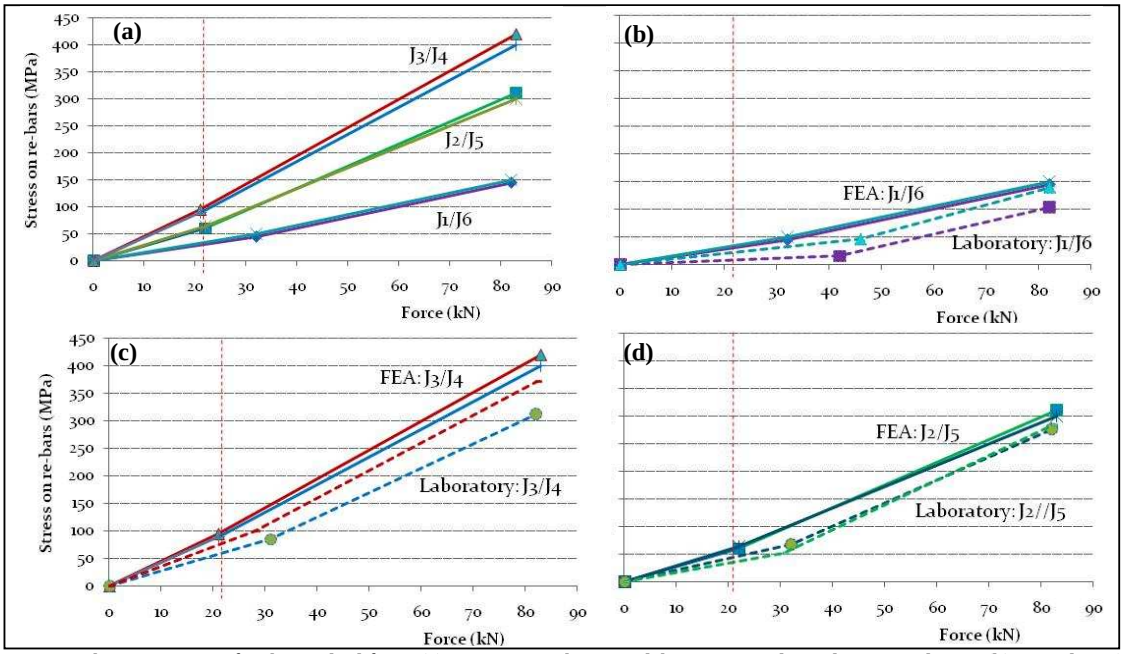

Fig. 7 Stress in each strain gauges for the applied force (a); comparison between laboratory results and numerical FEA (b) J3 and J4, (c) J2 and J5, and (d) J1 and J6

The strain distribution patterns observed in the FEA are similar with the experimental results. By comparing Fig. 8 and Fig. 4(b) it can be observed that strain distribution at each end of the bar shows close resemblance between FEA and experimental.

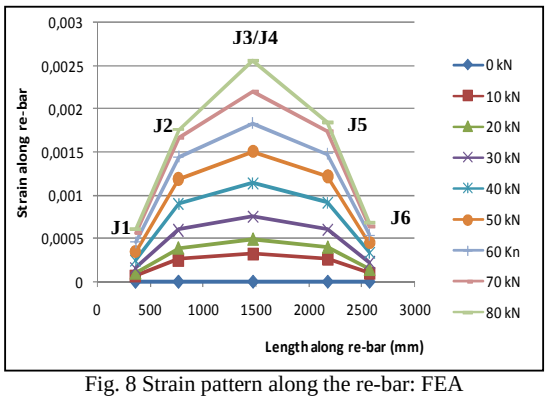

Fig. 8 Strain pattern along the re-bar: FEA

For the maximum load of 80kN, both ends of the re-bar have strain around 0.0006. This is where the J1 and J6 located. For the location of J2 and J6, strain recorded in the experimental works is around 0.0014 as compare to FEA; 0.0016. The strain pattern in the center of the beam for FEA is higher than laboratory results; 0.0025 as compare to 0.0018.

IV. Conclusions

From the study conducted on inoxydable steel bar, it can be conclude that the experimental concept for the bending test on simply supported beam is able to observe and record the tension stiffening phenomenon in concrete composite. Tension stiffening parameters used is acceptable and the modeling strategies made in ABAQUS can closely represent the actual condition.

References

[1] Ali Nour, Bruno Massicotte, Emre Yildiz, and Viacheslav Koval, Finite element modeling of concrete structures reinforced with internal and external fibre-reinforced polymers, Can. J. Civ. Eng. 2007; 34: 340-354.

[2] B. Winkler, G. Hofstetter, and H. Lehar, Application of a constitutive model for concrete to the analysis of a precast segmental tunnel lining, Int. J. Numer. Anal. Meth Geomech. 2004; 28: 797-819.
[3] EN 1992-1-1. Eurocode 2 - Design of concrete structures, Part 1.1, General rules and rules for buildings. CEN; 2003.
[4] H. Sooriyaarachchi, K. Pilakoutas, and E. Byars, Tension stiffening behavior of GFRP-reinforced concrete, 7th International Symposium on Fiber Reinforced Polymer Reinforcement for Reinforced Concrete Structures (FRPRCS-7), November 6-10, 2005, Kansas City, Missouri.
[5] Rim Nayal and Hayder A. Rasheed, Tension stiffening model for concrete beams reinforced with steel and FRP bars, Journal of Materials in Civil Engineering 2006; 18(6): 831-841.
[6] Abaqus Analysis User's Manual, Version 6.4. U.S.A: ABAQUS, Inc., 2003.